2026 IEEE International Conference on Robotics and Automation (ICRA 2026)
June 1-5, 2026. Vienna, Austria

A Tactile Rubbing Gripper for Reliable Fabric Separation

Zhengrong Ling[1#], Zhenghao Huang[1#] and Yajing Shen[1*]

***Abstract*— Automated fabric manipulation offers great potential for reducing labor requirements in textile manufacturing and domestic services. Yet, even the basic task of separating a single fabric layer poses substantial challenges for robots. Adhesive-based end-effectors suffer from limited material compatibility and environmental adaptability, while gripper-based designs, which primarily target crease grasping and rely on passive separation, frequently demonstrate unreliability. Current vision and tactile systems fail to detect the fabric separation surface. Given these mechanical and sensing constraints, existing separation solutions lack the ability to adjust the number of layers post-grasping, relying solely on single-attempt success. In this work, we propose a novel tactile-enhanced gripper capable of human-like rubbing motion for reliable cloth separation, which integrates a magnetic sensing system to monitor the separation process. Based on these, we further develop a pipeline to realize rubbing-based separation. Extensive experiments show our gripper achieves a 96.67% separation success rate across 15 fabrics with varying weaving patterns, and the tactile system reaches 87.00% accuracy in sliding surface detection. Our work provides a novel mechanism for fabric layer separation, facilitating subsequent cloth manipulation.**

I. Introduction

Automated fabric manipulation holds significant importance in reducing labor intensity in the textile industry and household services, being a long-term pursuit of humans. The fabric manipulation involves many operations, such as flattening, folding, and unfolding, many of which have been highly automated [1], [2], [3], [4], [5], [6]. However, the most fundamental and common operation—separating a single layer of fabric from a stack—remains difficult to automate due to insufficient fine fabric handling ability. This limitation hinders the application of existing robotic technologies and full automation in fabric manipulation.

To address this issue, various end-effectors based on different principles have been proposed. Some studies have explored top-layer fabric separation strategies using adsorption or adhesion methods, including suction cups [7], [8], [9], micro-needles [10], [11], and electro-adhesion [12], [13]. However, the adhesion performance of these methods is affected by fabric material, texture, temperature, and humidity, which greatly limits their applicability. A more natural alternative is to clamp the top fabric layer using two or more fingers. Based on this principle, some studies use non-rolling fingers to pinch fabrics [14], [15], which requires first pressing the fabric to create creases—limiting their applicability to soft fabrics. Some grippers with rolling fingers have also been designed, enabling the rolling up or adjustment of objects [16], [17], [18], [19]. However, these solutions do not actively separate fabrics; picking a single layer relies heavily on passive fabric separation (i.e., the underlying fabric separates from the top layer by gravity when the top layer is pinched), resulting in unrobust separation.

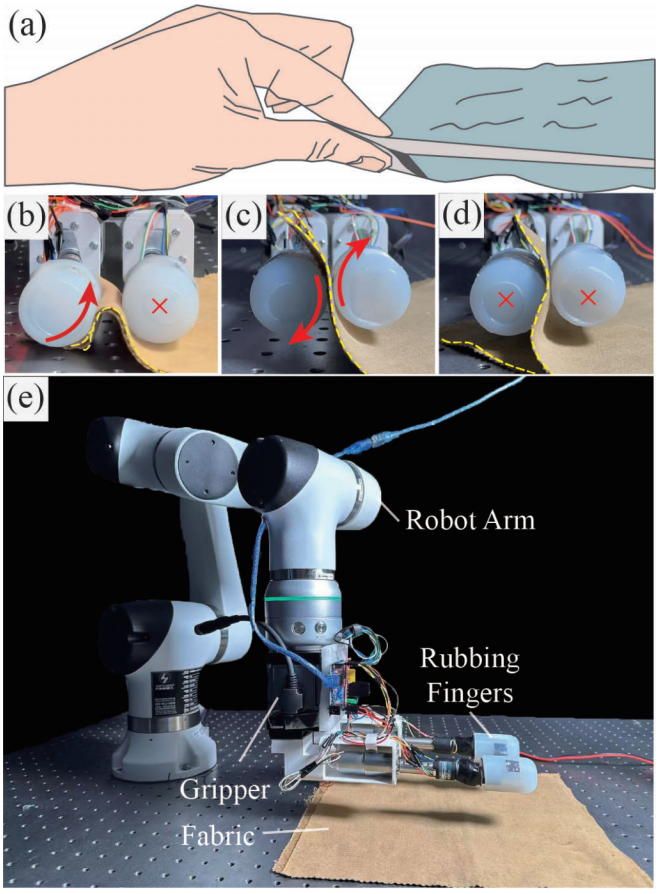

Fig. 1: The tactile rubbing gripper inspired by humans. (a) Human fabric layer separation (b)-(d) Fabric manipulation via tactile rubbing grippers. (e) Fabric separation system.

[#]These authors contributed equally to this work

[1]Zhengrong Ling and Zhenghao Huang are with the Department of Electronic and Computer Engineering, the Hong Kong University of Science and Technology, Kowloon, Hong Kong. Yajing Shen is with the Department of Electronic and Computer Engineering, Research Center on Smart Manufacturing, and the Cheng Kar-Shun Robotics Institute, the Hong Kong University of Science and Technology, Kowloon, Hong Kong. E-mails: zlingab@connect.ust.hk, zhuangdz@connect.ust.hk, eeyajing@ust.hk. This research was funded by Guangdong Basic and Applied Basic Research Foundation (2023B1515130007), National Natural Science Foundation of China / Research Grants Council Joint Research Scheme (N_HKUST638/23, 62361166630), ShenZhen Key Basic Research Project (JCYJ20241202124427037), and Hong Kong RGC General Research Fund (16217424).

TABLE I: Summary of Separation Solutions & Characteristics

Solution		Temperature Humidity Robust	Crease-free	Separation Principle	Sliding Sensing	Adjustment after Picking
Adsorption /Adhesion	Suction Cups	No	/	Passive	No	No
	Micro-needles	No	/	Passive	No	No
	Electro-adhesion	No	/	Passive	No	No
Clamping	Pinch	Yes	No	Passive	No	No
	Rolling	Yes	Yes	Passive	No	No
	Rubbing (ours)	**Yes**	**Yes**	**Active**	**Yes**	**Yes**

In addition to the gripper mechanism, sensing capabilities for monitoring the separation states are also critical for generating actions to reliably separate. Vision-based solutions represent the most straightforward approach to acquiring feedback. Such methods identify suitable manipulation positions from captured images [20], yet fail to determine whether the fabrics are separated, as they are inherently limited by visual occlusion.

In contrast, tactile sensing offers a more effective solution for detecting separation states: during finger-fabric contact, contact forces are converted into visual or magnetic tactile signals, which are then processed to count fabric layers [21], perceive local contact events [22], or control contact forces [23]. However, these sensing solutions cannot effectively monitor the core separation state—i.e., whether the fabrics have been successfully separated from each other. Thus, the feasibility of using tactile sensors to detect the occurrence of fabric separation has yet to be conclusively validated.

Therefore, existing end-effectors cannot actively separate objects after picking due to the lack of dedicated mechanisms and effective sensing, relying solely on a single successful pick. To fill this gap, we propose a novel gripper that achieves active fabric separation through rubbing and detects the separation state via tactile sensing. Our contributions are as follows.

1) A mechanical solution for fabric separation: We design a mechanical solution capable of active rubbing to achieve fabric separation, achieving an overall 96.67% success rate across 15 different types of fabrics.

2) A tactile solution for fabric separation detection: We design a tactile sensing solution, achieving an overall 87% accuracy in fabric separation detection across 15 fabric types.

3) A strategy for robust separation: We propose an automated pipeline for robust fabric separation, which has been successfully validated through real-world experiments.

II. Principle & Design

To separate a single layer of fabric, humans intuitively perform a rubbing motion, as shown in Fig. 1(a), and perceive the difference between fabric–fabric sliding and hand–fabric sliding. Once only one fabric layer remains, relative sliding occurs between the hand and the fabric, allowing humans to stop immediately and pick up the single layer.

By mimicking this mechanism, this study designs a gripper that generates rubbing motions through rotation, thereby realizing fabric separation via active rubbing. Meanwhile, we develop a tactile sensing scheme based on magnetic field variation detection, which, combined with a neural network, enables the perception of sliding states. Furthermore, by integrating the rubbing motion and sliding detection, we design a fabric separation pipeline featuring "gripping–feedback–active correction" for reliable single-layer isolation.

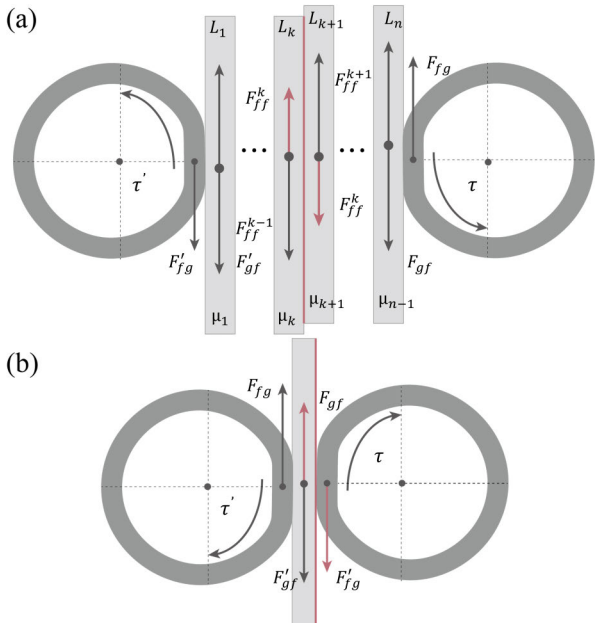

Fig. 2: Analytical Model of Fabric Separation. (a) Rubbing multiple layers of fabric. (b) Rubbing a single layer.

A. Rubbing Separation

The separation process can be modeled through force analysis of the fabric stack. When the gripper pinches n layers of fabric, as shown in Fig. 2(a), the fabrics maintain equilibrium under the action of friction, with the conditions as follows:

$$F'_{\mathrm{gf}} = F^1_{\mathrm{ff}} = \cdots = F^k_{\mathrm{ff}} = \cdots = F^{n-1}_{\mathrm{ff}} = F_{\mathrm{gf}} \tag{1}$$

where n is the number of layers. The F'_{gf} and F_{gf} are the friction provided by the left and right fingers on the fabrics, respectively. F^k_{ff} is the friction generated on the surface between layer L_k and L_{k+1}.

Once the torques of the motors τ increase, the friction between the fingers and the fabric F_{gf}, as well as between the fabrics F_{ff}, will correspondingly increase until the balance

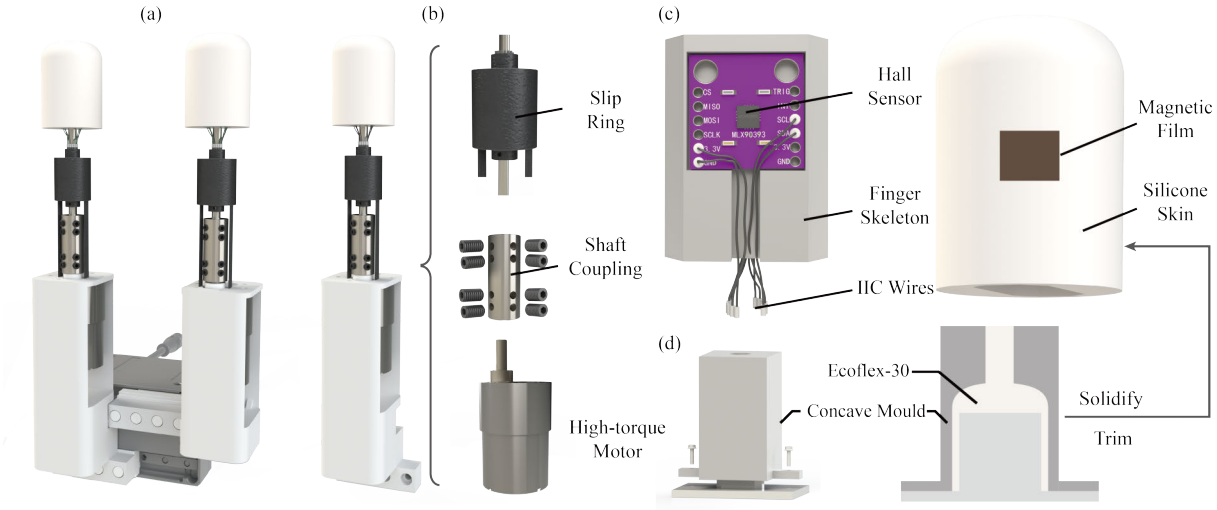

Fig. 3: (a) Tactile rubbing gripper. (b) Single-finger of tactile friction gripper. (c) Sensing structure on the fingertip, comprising a Hall-effect sensor mounted frame and silicone skin with magnetic coating. (d) Fabrication process of silicone skin.

is disrupted. If the friction between the fingers F_{gf} and the fabrics is guaranteed to be always greater than that between the fabrics F_{ff}, the critical point of separation occurs when an interface between the fabrics can no longer provide sufficient friction, i.e.

$$\begin{aligned} \mu_{\text{ff}}^{k} F_N < F_{\text{ff}}^{k+1} = \cdots = F_{\text{ff}}^{n-1} = F_{\text{gf}} \\ \mu_{\text{ff}}^{k} F_N < F_{\text{ff}}^{1} = \cdots = F_{\text{ff}}^{k-1} = F'_{\text{gf}} \end{aligned} \tag{2}$$

where μ_{ff}^{k} is the friction coefficient of the interface between layer L_k and L_{k+1} and the F_N is the normal force. At the moment of the separation, the cloth layers on each side of the separation interface will experience accelerations in distinct directions as follows:

$$a = \frac{1}{m}(F_{\text{gf}} - \mu_k F_N),\ a' = \frac{1}{m'}(F'_{\text{gf}} - \mu_k F_N) \tag{3}$$

Then, each parts of the fabrics speed up and catches up to the speed of the fingers.

After multiple separation rounds, the number of clamped fabric layers gradually decreases. In the final state where only one fabric layer remains, the scenario changes: the sole interface capable of relative sliding is that between the finger and the fabric, as shown in Fig. 2(b). Consequently, the fabric will either maintain a stationary position i.e.

$$a_1 = \frac{1}{m_1}(F_{\text{gf}} - F'_{\text{gf}}),\ F_{\text{gf}} \approx F'_{\text{gf}} \tag{4}$$

The design of the rubbing gripper is illustrated in Fig. 3. The system is based on a parallel gripper (Fig. 3(a)), which enables finger movement and fabric pinching. As shown in Fig. 3(b), each finger is driven by a motor through a transmission module, which delivers torque to a rotating fingertip. The fingertip adopts a soft cylindrical structure that rotates to generate the rubbing action on the fabric. The internal structure of the finger is detailed in Fig. 3(c). A rigid prismatic skeleton serves as the core structure, providing mechanical support and housing the sensing elements. Ecoflex-30 silicone—a widely used material with high friction—is selected as the finger skin to encapsulate the skeleton. The corresponding molding-based fabrication process is shown in Fig. 3(d). Since Ecoflex-30 is insensitive to environmental changes and maintains stable friction under varying humidity and temperature, the rubbing gripper achieves strong environmental robustness. Two tactile sensor modules are symmetrically integrated on opposite sides of the prism. Each sensor provides a 180° tactile sensing range, and their combined arrangement achieves full 360° tactile coverage around the finger circumference.

B. Tactile Sensing for Sliding Surface Detection

The tactile sensing system employs a magnetic-based architecture, comprising magnetized films, Hall sensors, and silicone encapsulation, as illustrated in Fig. 4. As shown in Fig. 4(a), the magnetic film is formed by stacking two layers of Halbach array magnetic films, each of which is sinusoidally magnetized. After stacking, the magnetic poles are periodically distributed along both in-plane directions, resulting in a unique three-dimensional magnetic field at each point in the 3D space near the magnetic film. This enables the detection of positional changes of the magnetic film caused by applied forces. As depicted in Fig. 4(b)-(c), the Hall sensors measure this field, outputting three digital signals corresponding to the magnetic field components along the X, Y, and Z axes. This configuration enables the system to detect both normal and shear contact forces. External forces deform the elastic silicone gel, displacing the embedded magnetic film and altering the magnetic field measured by the Hall sensors. Fig. 4(d) demonstrates the response to shear forces during fabric rubbing: the silicone skin undergoes tangential compression, shifting the magnetic film horizontally and producing a characteristic transformation in the magnetic

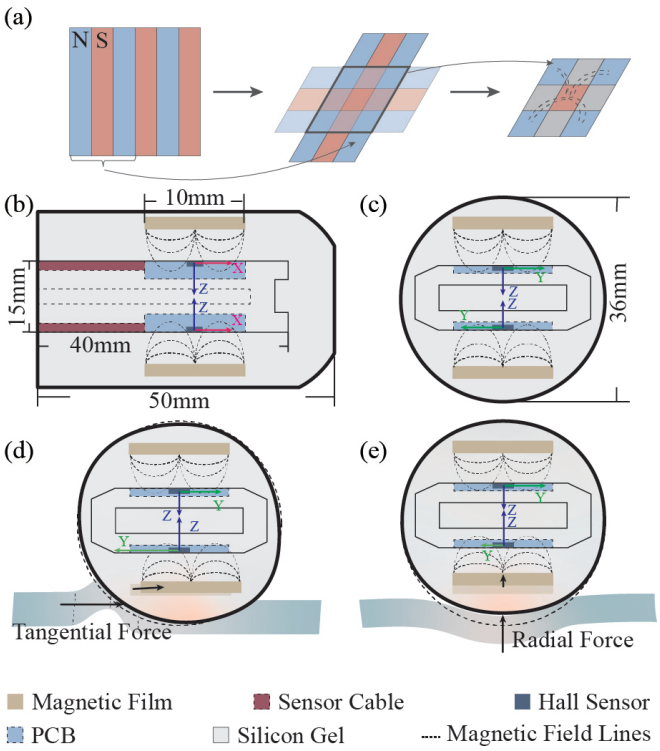

Fig. 4: The structure and principle of the tactile module. (a) Fabrication of the magnetic film (b) Cross-sectional view of the sensing module. (c) Unloaded state of the sensing module. (d) Tangential force applied to the sensing module. (e) Radial force applied to the sensing module

field readings. Conversely, as shown in Fig. 4(e), normal forces during fabric grasping cause radial compression of the silicone, resulting in vertical displacement of the magnetic film and a corresponding vertical transformation of the magnetic field measurements. These distinct signal patterns enable robust discrimination between different force types and magnitudes during manipulation tasks.

We used a neural network to identify sliding positions from tactile data. A sliding window processed 3D data of length N as one sample, labeled hand-fabric or fabric-fabric. To exploit temporal information, a Temporal Convolutional Network (TCN) mapped the $N \times 3$ sequence to labels.

C. Pipeline of Robust Fabric Separation

Based on the principle presented in Section II-A, multiple fabric layers can be separated via rubbing until only a single layer remains. By detecting the relative sliding between the finger and the single-layer fabric during recognition, the robot can reliably pick up the individual fabric layer

Accordingly, the proposed separation pipeline, outlined in Algorithm 1, is designed as follows: After initial pickup, the gripper executes a rubbing motion, while tactile data are processed in real time to localize the active sliding interface. This process iterates continuously as long as inter-fabric-layer sliding is detected. The action terminates when sliding is identified at the finger–fabric interface, a clear indicator that a single fabric layer has been isolated.

Algorithm 1 Separation of a Single Layer Fabric

Require: Tactile Data d_t, Trained Model f_θ, Tactile Data Queue Q_t, State Queue Q_s

Processor 1: Process data & detect the sliding state
loop
  $d \leftarrow [d_{t-9} : d_t] \leftarrow Q_t$
  $Q_s \leftarrow$ State $s_t = f_\theta(d),\ s_t \in \{0 : \text{H-F}, 1 : \text{F-F}\}$
end loop
Processor 2: Read data & generate action
loop
  Read d_t, and add d_t to Q_t
  $I_t = \prod_{i=t-9}^{t} s_i$
  if $I_t = 0$ **then**
    Set action $a_t = 0$: Stop the fabric separation process
  else if $I_t = 1$ **then**
    Set action $a_t = 1$: Rub to separate the layer fabrics
  end if
end loop

III. Experiment & Result

We conducted extensive physical experiments to evaluate the performance of the proposed tactile rubbing finger and pipeline for single-layer fabric separation. Physical rubbing tests under various conditions, sliding detection, and automated real-robot experiments were performed to investigate three key issues: (1) whether the proposed rubbing gripper can achieve the single-layer fabric separation task;(2) whether the proposed sensing scheme can effectively and accurately perceive the sliding state;(3) whether the proposed single-layer fabric separation pipeline can realize reliable single-layer separation.

A. Friction Calibration & Experimental Setup

In our experiments, 15 types of fabrics were employed (see Fig. 5), covering 2 weaving methods and 9 material compositions. Notably, the friction coefficient differs with variations in weaving techniques and fabric materials.

The sliding friction coefficients between fabric–fabric and fabric–silicone were first measured, as shown in Fig. 6(a)–(b). A force sensor (20 N range, 0.5% accuracy, 0.001 N resolution) was adopted. Five repeated tests were conducted for each condition, with mean values used for analysis.

As shown in Fig. 6 with standard deviations, the friction coefficient ranges from 6.08×10^{-4} to 34.84×10^{-4}, while the silicone-fabric friction coefficient ranges between 24.97×10^{-4} and 45.59×10^{-4}. Importantly, the silicone-fabric friction coefficient is consistently higher, which supports the effectiveness of rubbing to separate fabric layers.

We fixed the gripper opening position and set the finger rotation speed to 32 degrees per second. The fabric was placed flat on the table, and the robot was pre-positioned at the designated fabric separation location. The fabrics were then rubbed toward the gripper using a set of fixed operations to facilitate subsequent separation.

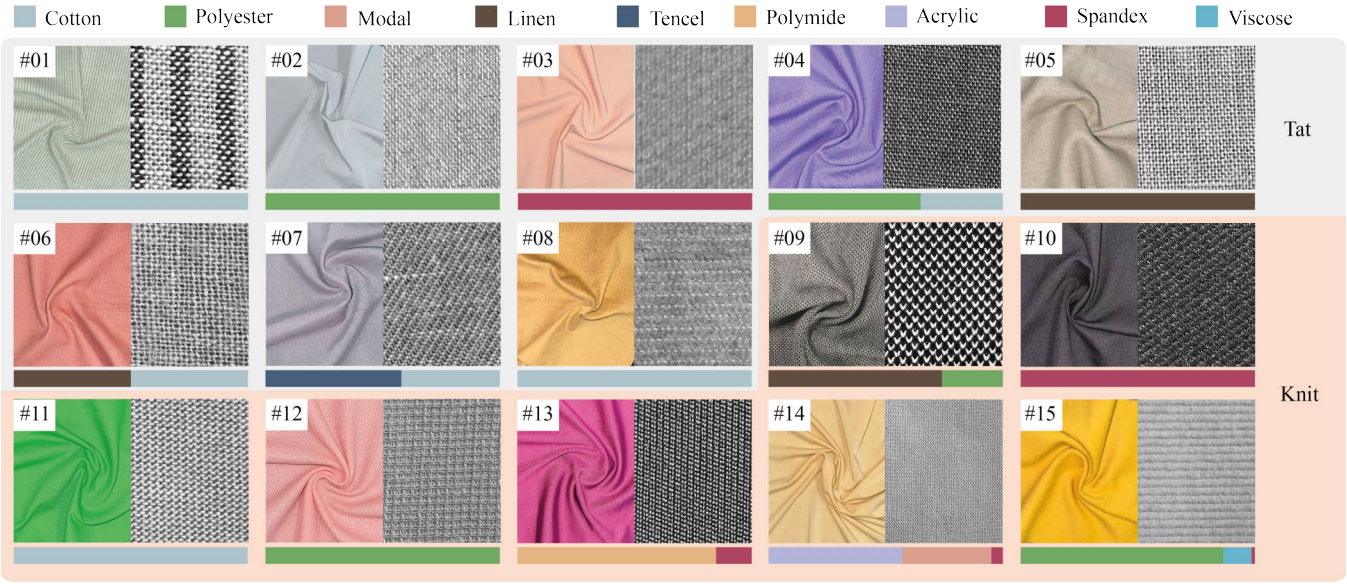

Fig. 5: Fabrics and serial numbers for experiments. Color bars show material composition and proportions.

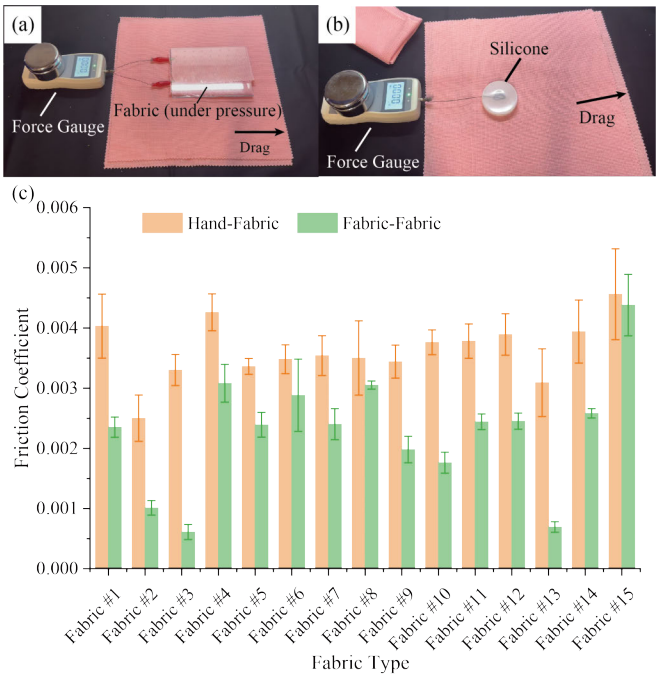

Fig. 6: Two types of friction coefficients. (a)–(b) are the measurement setups. (c) shows friction coefficients.

B. Rubbing Mechanism

In this section, we performed comprehensive tests on the proposed gripper for the fabric separation task, as illustrated in Fig. 7. The separation procedure comprises six sequential phases: approaching fabrics, rubbing up, pinching multiple layers, rubbing down, pinching a single layer, and completing separation. A test is deemed successful only if the gripper reliably accomplishes the pinching a single layer phase.

Table II summarizes the separation success rates under different layer counts. The results demonstrate excellent performance of the proposed gripper, achieving a 100% overall success rate for 6 types of fabrics. For other fabrics with diverse material compositions and weaving methods, the system maintains an overall success rate of over 90%. Failures occurred because the gripper only performed preset clamping without constant force control, causing the fabric to drop before rubbing. As shown in the table, the number of layers has a negligible influence on separation performance, with success rate variations across layer counts of less than 30.00%. The overall success rate across all fabric types and layer numbers is 96.67%. Although this study only evaluated single-layer separation of the same fabric type among 15 fabrics, the robotic fingertip material can be adaptively selected or modified to ensure hand-fabric friction exceeds that between different or identical fabric types, thereby expanding the applicable range of the gripper.

We recorded the time required to separate the fabric in a single attempt. Additionally, we used the gripper to perform one rub motion on 6 layers of fabric, repeating the process 10 times for each type of cloth, and recorded the average number of layers separated per attempt. The results are summarized in the Fig. 8. The result shows that the average time per separation is 8.11 seconds. The most time-consuming separation occurred with fabric #3 (10.26 seconds), while the shortest was 7.52 seconds with fabric #11. On average, each separation iteration removes 3.70 layers, indicating high operational speed.

We also conducted fabric separation tests on both the edges and corners of the cloth, as illustrated in Fig. 9. The results demonstrate that the gripper achieved a success rate of 93.33% in both scenarios (with 15 tests per condition).

C. Tactile Sensing & Sliding Surface Detection

For evaluating the sensing scheme's performance, we calibrated it, carried out sample analysis, and collected real rubbing data to test its success rate.

Fig. 7: The process of separating different fabrics using rubbing grippers.

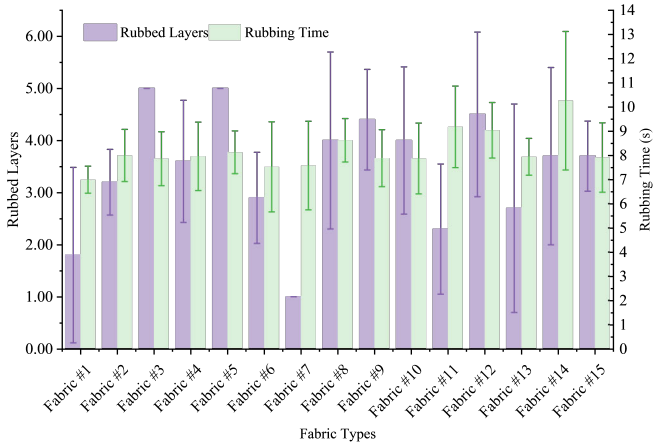

Fig. 8: Duration of one rubbing motion and number of layers separated per operation.

TABLE II: Separation Success Rate on Different Fabrics

Fabric Type	n=2	n=3	n=4	Overall
Fabric #1	10/10	7/10	10/10	90%
Fabric #2	9/10	10/10	10/10	96.67%
Fabric #3	10/10	10/10	10/10	100%
Fabric #4	10/10	10/10	9/10	96.67%
Fabric #5	10/10	10/10	10/10	100%
Fabric #6	10/10	10/10	10/10	100%
Fabric #7	10/10	10/10	10/10	100%
Fabric #8	10/10	9/10	10/10	96.67%
Fabric #9	10/10	10/10	10/10	100%
Fabric #10	10/10	10/10	10/10	100%
Fabric #11	9/10	9/10	10/10	93.33%
Fabric #12	9/10	10/10	10/10	96.67%
Fabric #13	8/10	10/10	10/10	93.33%
Fabric #14	7/10	10/10	10/10	90.00%
Fabric #15	9/10	10/10	10/10	96.67%

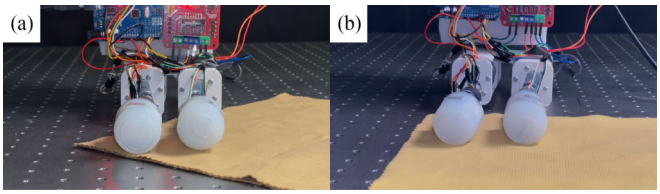

Fig. 9: Position for separation tests. (a) Test at the fabric corner. (b) Test at the fabric edge.

We calibrated the sensing signals induced by standard forces applied at different positions on the circular finger. The standard force was generated using a force gauge (accuracy: ±0.01 N; model: SC-5N; ShenCe, China). As shown in Fig. 10(a), the circular finger was divided into eight regions at 45° intervals starting from 0°. The application modes of tangential and radial forces are illustrated in Fig. 10(b)–(c), respectively. We first calibrated the effects of tangential and radial forces on the Y-axis and Z-axis outputs at the magnetic film location, as presented in Fig. 10(d)–(g).

In the normal force calibration experiment, a 0.2 N radial force was applied to each region. The readings from the two sensors integrated inside the finger are plotted in Fig. 10(d)-(e). The results indicate that the sensing system responds approximately linearly to force changes. In the tangential force calibration experiment, a 0.5 N tangential force was applied to each region. The Y-axis data collected by the sensing system are displayed in Fig. 10(f). The sensor outputs decreased as the loading position moved away from the magnetic film. Specifically, the sensor above the magnetic film yielded the maximum response, whereas the other sensor produced the minimum response. Each sensor covers a 180°

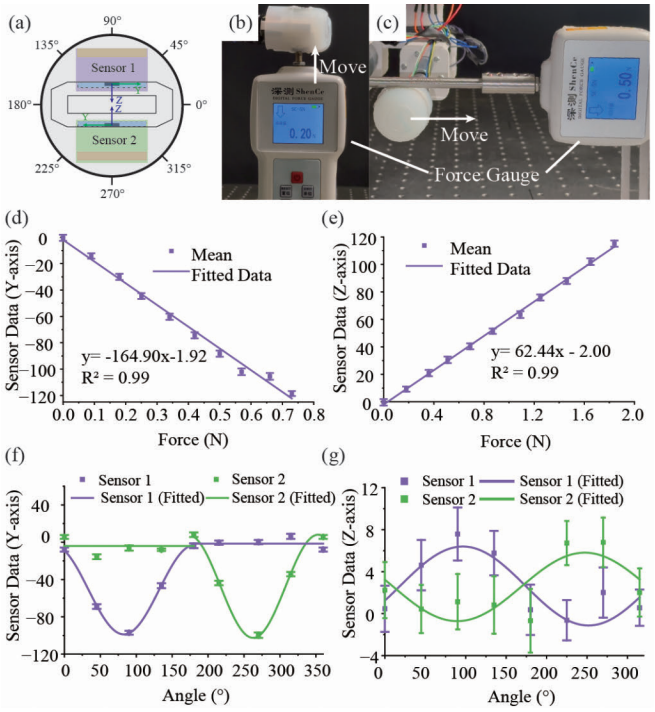

Fig. 10: Setups and results of sensor calibration. (a) Sample angles of the finger. (b)-(c) Setups of the calibration. (d) Y-axis data vs. tangential force. (e) Z-axis data vs. the radial force. (f) Y-axis data vs. tangential force positions. (g) Z-axis data vs. radial force positions.

sensing range, and the measured output decreases as the force application point moves away from the magnetic film. Fig. (g) shows the effect of tangential force position on the two sensors. The force position and sensor values follow a sinusoidal relationship. The sensor output is maximum when the force is directly above it.

To further validate the effectiveness of the sensing system in detecting sliding states, we collected data during rubbing operations and constructed a corresponding dataset. The dataset comprises rubbing signals acquired from 15 types of fabrics. For each fabric, sliding tests were carried out under three configurations: single-layer rubbing (hand–fabric sliding, H-F), double-layer rubbing (fabric–fabric sliding, F-F), and triple-layer rubbing (fabric–fabric sliding, F-F), with 30 trials performed for each configuration. Each recorded rubbing signal was segmented using a sliding window with a length of 10 and a step size of 1. Of the segmented samples, 30% were randomly selected as the test set. The model was trained for 50 epochs with a learning rate of 0.001 under the binary cross-entropy loss function.

The recall and accuracy metrics obtained in this study are detailed in Table III. The overall classification accuracy is 87.00%, among which the highest accuracy reaches 93.72%. It can be observed that ten types of fabrics achieve an accuracy rate higher than 85%, demonstrating the effectiveness of the proposed method in fabric recognition. Meanwhile, the overall recall values for the corresponding experimental

TABLE III: Detection Across Fabric Types and Layer Counts

Fabric Type	**H-F**	**F-F** ($n=2$)	**F-F** ($n=3$)	**Overall**
Fabric #1	83.61%	68.25%	93.77%	81.81%
Fabric #2	80.61%	77.99%	92.38%	82.90%
Fabric #3	89.09%	58.80%	94.16%	82.46%
Fabric #4	89.06%	64.92%	92.54%	84.21%
Fabric #5	88.25%	85.61%	97.21%	89.60%
Fabric #6	86.41%	90.37%	98.29%	90.32%
Fabric #7	87.62%	81.97%	92.35%	87.34%
Fabric #8	90.78%	83.58%	98.53%	90.58%
Fabric #9	86.53%	80.70%	94.55%	87.18%
Fabric #10	92.10%	92.03%	96.29%	93.10%
Fabric #11	85.07%	67.73%	97.61%	83.79%
Fabric #12	94.03%	90.57%	95.71%	93.72%
Fabric #13	86.82%	53.77%	93.68%	79.66%
Fabric #14	86.46%	90.08%	87.96%	87.75%
Fabric #15	86.05%	89.64%	99.05%	90.32%
Overall	87.61%	77.88%	94.80%	87.00%

settings are 87.61%, 77.88%, and 94.80%, respectively, further validating the reliability and stability of the detection system.

Furthermore, we investigate the tactile data throughout the entire separation process. As shown in Fig. 11, time-domain and frequency-domain analyses reveal that the tactile signals exhibit distinct characteristics when sliding on different surfaces.

D. Separation Pipeline

To validate the proposed fabric separation pipeline, we performed automated fabric separation experiments. As illustrated in Fig. 11, a robot integrated with a tactile rubbing gripper was employed to execute fabric separation. A total of five trials were conducted. The results show that the gripper can stably perform rubbing operations, with a sliding detection accuracy of 97% throughout the process. The robot successfully completed four of the five automated separation tasks, achieving an overall success rate of 80%.

IV. Conclusion & Discussion

In this work, we present a tactile-enhanced gripper capable of human-like rubbing for separating a single layer of fabrics. This active rubbing mechanism allows the gripper to reliably isolate individual layers without relying on passive separation of the fabric. Concurrently, a tactile sensing solution is proposed and integrated into the gripper, providing feedback of the sliding surface detection. The rubbing-based pipeline with post-picking adjustment has been validated as effective, enabling robots to generate actions based on sliding tactile feedback. Our work provides the community with a novel fabric separation mechanism.

Currently, this study only focuses on specific fabric types in the separation system; to extend its applicability to diverse fabrics, future research should expand the training dataset covering situations with more or mixed types of fabrics or explore the vibration mechanisms inherent in sliding friction. Furthermore, visual sensing can be added to extend automatic separation to the whole automatic fabric manipulation.

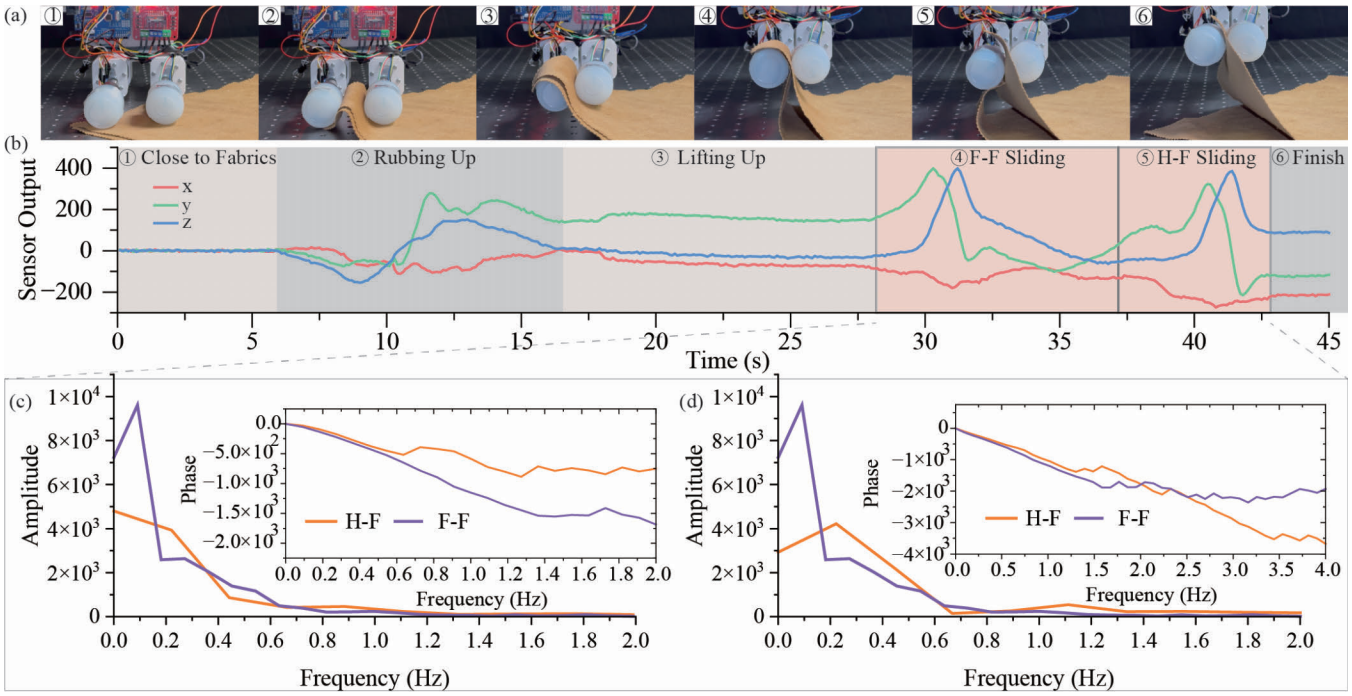

Fig. 11: Fabric separation and tactile data. (a) Separation process. (b) Tactile data during separation (left finger, one sensor). (c) Y-axis frequency characteristics. (d) Z-axis frequency characteristics.

REFERENCES

[1] C. Zhou, R. Jiang, F. Luan, S. Meng, Z. Wang, Y. Dong, Y. Zhou, and B. He, "Dual-arm robotic fabric manipulation with quasi-static and dynamic primitives for rapid garment flattening," *IEEE/ASME Transactions on Mechatronics*, 2025.

[2] L. Sun, G. Aragon-Camarasa, S. Rogers, and J. P. Siebert, "Accurate garment surface analysis using an active stereo robot head with application to dual-arm flattening," in *2015 IEEE international conference on robotics and automation (ICRA)*. IEEE, 2015, pp. 185–192.

[3] A. Doumanoglou, J. Stria, G. Peleka, I. Mariolis, V. Petrik, A. Kargakos, L. Wagner, V. Hlaváč, T.-K. Kim, and S. Malassiotis, "Folding clothes autonomously: A complete pipeline," *IEEE Transactions on Robotics*, vol. 32, no. 6, pp. 1461–1478, 2016.

[4] Y. Avigal, L. Berscheid, T. Asfour, T. Kröger, and K. Goldberg, "Speedfolding: Learning efficient bimanual folding of garments," in *2022 IEEE/RSJ International Conference on Intelligent Robots and Systems (IROS)*. IEEE, 2022, pp. 1–8.

[5] R. Proesmans, A. Verleysen, and F. Wyffels, "Unfoldir: Tactile robotic unfolding of cloth," *IEEE Robotics and Automation Letters*, vol. 8, no. 8, pp. 4426–4432, 2023.

[6] T. Lips, V.-L. De Gusseme, and F. Wyffels, "Learning keypoints for robotic cloth manipulation using synthetic data," *IEEE Robotics and Automation Letters*, vol. 9, no. 7, pp. 6528–6535, 2024.

[7] Z. Ma, H. Chen, D. Zhou, M. Ding, and X. Yue, "Research on fabrics stack separation and transfer method based on bernoulli suction cup non-contact grasping technology," *Journal of Engineered Fibers and Fabrics*, vol. 19, p. 15589250241260839, 2024.

[8] B. Ozcelik and F. Erzincanli, "A non-contact end-effector for the handling of garments," *Robotica*, vol. 20, no. 4, pp. 447–450, 2002.

[9] G. Dini, G. Fantoni, and F. Failli, "Grasping leather plies by bernoulli grippers," *CIRP annals*, vol. 58, no. 1, pp. 21–24, 2009.

[10] S. Ku, J. Myeong, H.-Y. Kim, and Y.-L. Park, "Delicate fabric handling using a soft robotic gripper with embedded microneedles," *IEEE Robotics and Automation Letters*, vol. 5, no. 3, pp. 4852–4858, 2020.

[11] S. Ku, B.-H. Song, T. Park, H.-Y. Kim, and Y.-L. Park, "Multifunctional soft gripper with microneedles and integrated sensing for robotic fabric handling," *IEEE/ASME Transactions on Mechatronics*, vol. 29, no. 2, pp. 866–877, 2023.

[12] H. He, G. Saunders, and J. T. Wen, "Robotic fabric fusing using a novel electroadhesion gripper," in *2022 IEEE 18th international conference on automation science and engineering (CASE)*. IEEE, 2022, pp. 2407–2414.

[13] K. M. Digumarti, V. Cacucciolo, and H. Shea, "Dexterous textile manipulation using electroadhesive fingers," in *2021 IEEE/RSJ International Conference on Intelligent Robots and Systems (IROS)*. IEEE, 2021, pp. 6104–6109.

[14] E. Ono and K. Takase, "On better pushing for picking a piece of fabric from layers," in *2007 IEEE international conference on robotics and biomimetics (ROBIO)*. IEEE, 2007, pp. 589–594.

[15] A. Seino, F. Tokuda, A. Kobayashi, and K. Kosuge, "Passive actuatorless gripper for pick-and-place of a piece of fabric," *IEEE/ASME Transactions on Mechatronics*, 2025.

[16] K. Manabe, X. Tong, and Y. Aiyama, "Single sheet separation method from piled fabrics using roller hand mechanism," in *2021 IEEE international conference on intelligence and safety for robotics (ISR)*. IEEE, 2021, pp. 359–362.

[17] J. Unde, J. Colan, and Y. Hasegawa, "Design, modelling, and experimental verification of passively adaptable roller gripper for separating stacked fabric," *IEEE Robotics and Automation Letters*, 2024.

[18] K. Yamazaki and T. Abe, "A versatile end-effector for pick-and-release of fabric parts," *IEEE Robotics and Automation Letters*, vol. 6, no. 2, pp. 1431–1438, 2021.

[19] S. Yuan, S. Wang, R. Patel, M. Tippur, C. L. Yako, M. R. Cutkosky, E. Adelson, and K. Salisbury, "Tactile-reactive roller grasper," *IEEE Transactions on Robotics*, 2025.

[20] Y. Kawasaki, S. Arnold, and K. Yamazaki, "Picking of one sheet of cotton cloth by rolling up using cylindrical brushes," in *2021 IEEE/SICE International Symposium on System Integration (SII)*. IEEE, 2021, pp. 54–59.

[21] S. Tirumala, T. Weng, D. Seita, O. Kroemer, Z. Temel, and D. Held, "Learning to singulate layers of cloth using tactile feedback," in *2022 IEEE/RSJ International Conference on Intelligent Robots and Systems (IROS)*. IEEE, 2022, pp. 7773–7780.

[22] C. Zhao, C. Jiang, L. Luo, S. Yuan, Q. Chen, and H. Yu, "Learning thin deformable object manipulation with a multi-sensory integrated soft hand," *IEEE Transactions on Robotics*, 2025.

[23] J. Jiang, X. Zhang, D. F. Gomes, T.-T. Do, and S. Luo, "Rotipbot: Robotic handling of thin and flexible objects using rotatable tactile sensors," *IEEE Transactions on Robotics*, 2025.